Hindawi
International Transactions on Electrical Energy Systems
Volume 2023, Article ID 9830292, 1 page
https://doi.org/10.1155/2023/9830292

Retraction

Retracted: Nondestructive Testing of Coal Mine Wire Ropes Based on Magnetic Sensors

International Transactions on Electrical Energy Systems

Received 12 December 2023; Accepted 12 December 2023; Published 13 December 2023

This article has been retracted by Hindawi, as publisher, following an investigation undertaken by the publisher [1]. This investigation has uncovered evidence of systematic manipulation of the publication and peer-review process. We cannot, therefore, vouch for the reliability or integrity of this article.

Please note that this notice is intended solely to alert readers that the peer-review process of this article has been compromised.

Wiley and Hindawi regret that the usual quality checks did not identify these issues before publication and have since put additional measures in place to safeguard research integrity.

We wish to credit our Research Integrity and Research Publishing teams and anonymous and named external researchers and research integrity experts for contributing to this investigation.

The corresponding author, as the representative of all authors, has been given the opportunity to register their agreement or disagreement to this retraction. We have kept a record of any response received.

References

[1] Y. Yuan, K. Wang, B. Chen, and Y. Qiu, "Nondestructive Testing of Coal Mine Wire Ropes Based on Magnetic Sensors," *International Transactions on Electrical Energy Systems*, vol. 2022, Article ID 1066163, 13 pages, 2022.

Hindawi
International Transactions on Electrical Energy Systems
Volume 2022, Article ID 1066163, 13 pages
https://doi.org/10.1155/2022/1066163

Research Article

Nondestructive Testing of Coal Mine Wire Ropes Based on Magnetic Sensors

Youliang Yuan,[1,2] **Kaihui Wang**,[1] **Baoyuan Chen**,[1] **and Yu Qiu**[1]

[1]*Tiandi (Changzhou) Automation Co., Ltd, Changzhou 213015, Jiangsu, China*
[2]*Power Engineering, Changzhou University, Changzhou 213015, Jiangsu, China*

Correspondence should be addressed to Youliang Yuan; youliangyuan@stu.cu.edu.kg

Received 4 August 2022; Revised 20 August 2022; Accepted 6 September 2022; Published 12 October 2022

Academic Editor: Raghavan Dhanasekaran

Safety is the first priority in production. The situation is complex in the deep underground of coal mines, and safety accidents often occur. Wire rope is a kind of safety device. With the help of wire rope, the safety of miners can be guaranteed to a certain extent. It is a very important tool for mining production. However, the current detection of coal mine wire rope still relies on the data from the factory, and it is impossible to achieve nondestructive testing in use. This article aims to study the degree of wear of mining wire ropes to ensure the safety of miners as much as possible. According to the characteristics of the wire rope, any defect (rust, broken wire, broken wire, etc.) changes in the cross-sectional area of the wire rope will change the magnetic permeability of the wire rope. With the help of equipment, we can collect data on changes in the magnetic field (MF). Based on this experimental design, the steel wire rope is given an MF, and the magnetic sensor is used to monitor the MF signal and convert it into an electrical signal. According to the collected electrical signal analysis and judgment, the sensor model is constructed, the size and position of the wire rope cross-sectional change are deduced, and the defect of the wire rope is judged. The experimental results in this study show that the magnetic sensor is an effective measure to monitor the nondestructive degree of the wire rope, with a sensitivity of more than 80%.

1. Introduction

The steel wire rope is a helical wire bundle, in which the steel wires whose mechanical properties and geometric dimensions meet the requirements are twisted together according to certain rules. The steel wire rope is composed of steel wire, rope core, and grease. As a highly conductive member with high resistance to traction, steel wire rope has been widely used in mines. Coal industry equipment, such as lifting, traction, extraction, and excavation equipment, are inseparable from the shadow of steel wire rope. In the production process of the coal mine, the mine hoisting wire rope is mainly used for the transportation of underground materials and personnel. Due to long-term work and frequent use, wire ropes often break wires in places where stress is concentrated. With the increase in the number of broken wires, once the two ends of the wire rope are impacted by a greater load, the entire wire rope will break, which will lead to accidents in the mine and seriously affect the safety of normal production line workers. Therefore, the research on new technologies and methods for detecting wire rope defects is particularly important. Some coal mines and wire rope users have always conducted relevant research on wire rope defect monitoring. However, due to the particularity of the steel wire rope structure and the complexity of the working environment, as a short board for the development of the coal industry, it is subject to tension, bending, twisting, and corrosion during the stress process, and it is susceptible to a variety of uncertain loads and harsh conditions. The influence of environmental factors makes the detection of wire rope defects extremely difficult. At present, a complete set of detection theories and detection methods have not been formed to meet the actual detection requirements of coal mine sites.

Because of the actual needs of industrial production, domestic and foreign experts and scholars have conducted a series of in-depth studies on the detection of steel wire ropes.

Wang et al. researched and proposed a new magnetic gathering bridge detection method using magnetoresistive sensor arrays, which solves the shortcomings of the current methods used to test the integrity of steel wire ropes used in coal mine operations [1]. Trinidad found a method for in-situ wire rope inspection using MFL. This method is well known and recognized in the following applications: lifting and balancing ropes in deep wells, ropeways, steel reinforced conveyor belts, wire ropes, ship lifts, crane cables, and elevator cables. The key to the MFL detection method is the loss of metal cross-sectional area (LMA) material loss area [2]. TOM achieves the purpose of eliminating risks and uncertainties by studying the residual magnetic field MFL-wire rope detection [3]. Zhou et al. proposed a new detection method based on the common wire rope in the market. His method is based on the texture of the wire rope, which can effectively identify the surface features of the wire. He proved the effectiveness of his method by testing common steel wires [4]. Tian et al. tracked the change of the failure date of the steel wire rope, and by comparing and observing the broken chain, the dry core, and the broken end mark of the steel wire rope, it was confirmed that the steel wire rope fracture was caused by fatigue [5]. Taking into account safety factors, pulley diameter, rope diameter, pulley shape factor, working load, and metal area, he suggested that the appropriate bending fatigue schedule of the wire rope should be changed from 9 months to 6 months [6]. Byoungjoon's magnetic flux leakage (MFL)-based detection system is used to diagnose the pressure deformation of steel wire ropes. He designed and manufactured a 4-channel MFL sensor head. Experiments have verified the feasibility of the wire rope damage detection technology [7]. Fontanari et al. have carried out research on lightning damage of aerial ropeway full-lock steel ropes. Through the measurement of single-wire mechanical degradation and a detailed study of its metallurgical modification, they discovered the microstructural properties of the mechanical damage, the strong directionality of the thermal shock effect and the localized damage of the outer layer of the fully locked rope [8]. Tian et al. investigated the impact of various prebroken wire distributions on the bending fatigue behavior of steel wire ropes using homemade bending fatigue test equipment. The fatigue life of steel wire ropes with various prebroken wire distributions was investigated using eye examination, commercial nondestructive testing methods, and electron microscopy. The bending fatigue life of the wire rope is observed to be shorter when there are broken wires on the surface. The wire break increases the contact force between the wires as well as the tension in the inner strands [9]. When the quantity of prebroken wires is most concentrated (14), this results in severe wear concentration, local acceleration of broken wire density, and short fatigue life. After the failure of many wires due to wear and fatigue, other wires will fail due to stretching overloads, such as necking and microscopic evidence of ductile failure [10]. These studies have expanded the wear causes and detection methods of steel wire ropes from different angles. The applicability and reliability of detection technology are not strong, the quantitative detection of steel wire rope metal cross-sectional area damage is lacking, and the safety evaluation methods and versatility of steel wire ropes are not perfect, resulting in steel wire ropes. Security problems still exist, and waste is serious.

This study uses MF to conduct nondestructive testing of steel wire ropes and draws on the relevant experience of domestic and foreign experts. This study designs a magnetic sensor for nondestructive testing of steel wire ropes. After many simulation tests, the experimental results show that the data are authentic and accurate, and the method is feasible, High sensitivity can be used for wire rope detection for various purposes such as mines. The innovation of this study is that in the nondestructive testing, this study adds the detection of the residual strength of the wire rope to the detection of the magnetic sensor, which can more accurately judge the damage of the wire rope.

2. Principles and Methods of Wire Rope Nondestructive Testing

2.1. Wire Rope Structure and Defect Analysis. The steel wire rope has high strength, lightweight, stable operation, and reliable operation and is not easy to break suddenly. The parts that make up the steel wire rope mainly include steel wire, rope strands, and rope core [11], as shown in Figure 1. The steel wire made of high-quality high-carbon steel has high strength due to repeated cold drawing and heat treatment. In order to improve the toughness and elasticity of the wire rope, the rope core is used to reduce friction and increase the life. The structural characteristics of the steel wire rope determine that it has the characteristics of good winding, high strength, lightweight, stable work, not easy to break suddenly, and reliable work [12].

There are various reasons for wire rope damage. The manifestations on the wire rope can be divided into two types: local damage type and metal cross-sectional area damage type. These two types can be abbreviated as LF type injury and LMA type injury according to their English. LF type damage is shown in Figure 2. The main damage type is broken wire, including bending fatigue broken wire, tension and tension overload broken wire, shear broken wire, wear broken wire, and rust broken wire [13]. LMA type damage is mainly caused by wear, aging, and corrosion.

A large number of actual survey results show that more than 80% of wire rope fractures are caused by fatigue damage. The fatigue damage of the wire rope brings huge hidden dangers to the normal use and personal safety of the wire rope.

2.2. Nondestructive Testing Technology. Nondestructive testing is to use the optical, electrical, magnetic, and acoustic characteristics of the tested object to detect whether there are defects or damages in the tested object and give the defect or loss under the premise of not affecting the normal use performance of the tested object and information on location, size, nature, and quantity. Nondestructive testing is a new development direction and an important supplement to destructive testing. Wire rope nondestructive testing

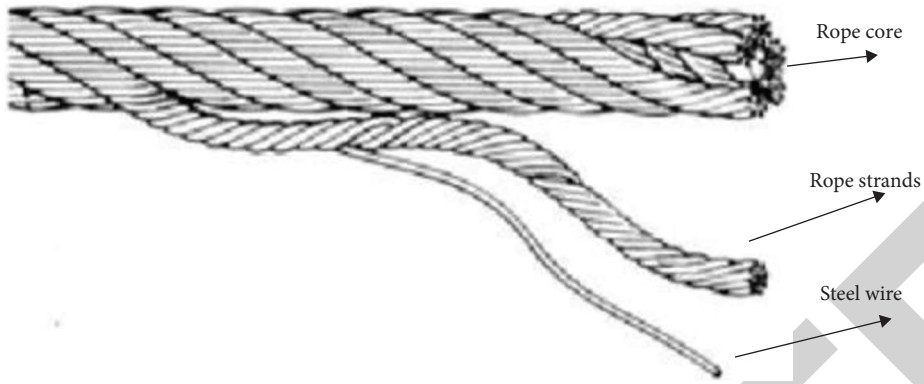

Figure 1: Wire rope structure.

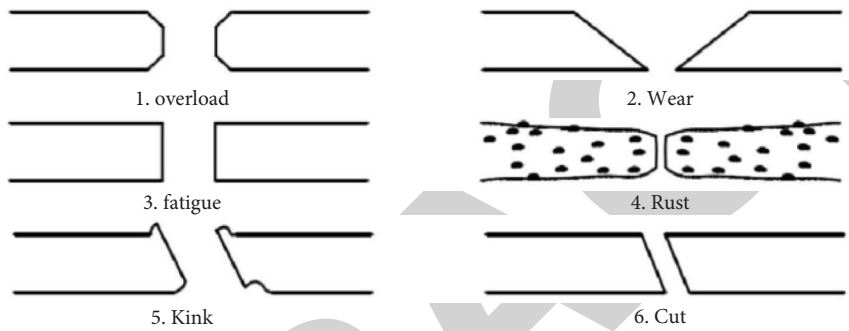

Figure 2: Types of LF loss.

methods can be divided into mechanical testing methods, radiographic testing methods, current testing methods, optical testing methods, ultrasonic testing methods, vibration testing methods, acoustic emission testing methods, and magnetic testing methods according to different testing principles [14, 15]. Nondestructive testing is an indispensable and effective tool for industrial development. To a certain extent, it reflects the level of industrial development of a country. The importance of nondestructive testing has been recognized.

Among these methods, the electromagnetic detection method of wire rope has been widely used because of its many advantages such as high sensitivity, good reliability, and low cost. It has great advantages in nondestructive detection of wire rope. Commonly used electromagnetic detection methods mainly include the magnetic flux leakage method, magnetic Barkhausen noise method, magneto-acoustic emission method, metal magnetic memory method, and eddy current detection method.

2.2.1. Magnetic Flux Leakage Detection Method. The primary detection principle of the magnetic flux leakage detection method is magnetizing the workpiece (close to fullness) and using the excitation device to excite the wire rope to induce an MF inside the wire rope. If the wire rope is intact, the magnetic flux is blocked inside the wire rope; if the wire rope fails, the magnetic flux will leak out. Sensors or induction coils are used to pick up the leaked MF and analyze the characteristics of the MF to get the fault information of the wire rope.

2.2.2. Magnetic Memory Testing Method. The magnetic memory detection method is essentially a special kind of magnetic flux leakage detection. It detects the own MF generated by the steel wire rope under the influence of the geomagnetic field during the manufacturing process, then converts the surrounding or internal MF information of the wire rope into electrical signals, and analyzes the wire rope characteristic signals through computer processing technology to determine whether there is damage.

2.2.3. Eddy Current Testing Method. The eddy current testing method uses AC induction coils to induce eddy currents on the surface of the wire rope, which will change when encountering defects, so as to detect whether the wire rope is defective or not. The detection principle of the eddy current detection method is relatively mature. When the transmitter coil is connected to a fixed frequency alternating current, an alternating primary MF will be generated around the coil. When approaching the wire rope, eddy currents are generated by electromagnetic induction inside the wire rope. The eddy currents generate alternating secondary MFs inside and around the wire rope, and the secondary MF induces a secondary current in the receiving coil. If there is a defect in the wire rope, the flow of eddy

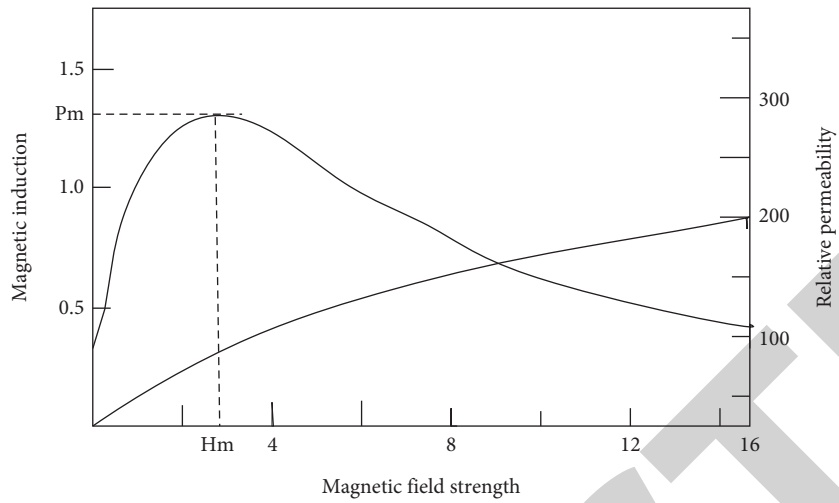

Figure 3: Magnetization characteristic curve.

current will be distorted to affect the secondary MF, which in turn affects the change of the induced current in the receiving coil, and the degree of the defect is judged by analyzing the changed current.

2.3. Magnetization Characteristics of the Wire Rope. Figure 3 shows a graph showing the magnetization characteristic curve of ferromagnetic material and the change of magnetic permeability with the intensity of the MF. According to the figure, the magnetization design of ferromagnetic materials can be carried out.

In the figure, the left part of the broken line is the weak magnetization. In this case, the relative magnetic permeability and magnetic induction intensity of the ferromagnetic material increase with the increase of the applied MF, and the response is more sensitive. In this case, the relative magnetic permeability has a larger value. If a defect occurs in a material, the MF in the adjacent material will increase, and the permeability will increase, so the magnetic flux leaking out of the air at the defect will decrease, which makes it difficult for the sensor to detect the defect. Pm is the point of maximum relative permeability of the ferromagnetic material, and point M is the MF strength when the permeability reaches the maximum value. In general, the relative permeability has a nonlinear relationship with the intensity of the material being magnetized, and its magnitude far exceeds the air gap permeability (1.000003–1.000004). In the part to the right of the dotted line in Figure 3, the leakage MF intensity caused by material defects increases with the excitation MF intensity. When the magnetization reaches the saturation zone, the magnetic induction intensity of the material changes slowly, and the MF intensity after 8 A/cm can be thought of it as a situation where the wire rope is in a strong magnetization [16]. In the case of deep excitation, the wire rope can no longer accept new magnetic induction lines, so the leakage MF will increase with the increase of the external MF, making the defect and fault easy to be detected by the sensor. It can be seen from the above analysis that in order to achieve the best magnetization effect when detecting the leakage MF, the wire rope should be magnetized to the deep saturation zone after the MF strength is 8 A/cm.

When a strong external MF is applied to the wire rope, the wire rope reaches a fully excited state. When the wire rope has a defect or failure, a part of the MF lines will escape into the air, which will interfere with the MF lines with relatively low density in the air. When this MF line reaches the surface of different magnetic mediums, there will be an escape phenomenon, which is called the refraction of MF lines. The above-mentioned escaped MF is the leakage MF [17]. Figure 4 shows the distribution of leakage MF of a classic wire rope broken wire defect fracture. Among them, Bx represents the horizontal component of the magnetic flux density of the leakage field, which is parallel to the magnetization direction; By represents the vertical component, which is perpendicular to the magnetization direction; l represents the depth of the defect; b represents the width of the defect. Therefore, in the detection, the position of the defect can be determined according to the position of the magnetic field change, and the wire rope can be processed quickly.

2.4. Residual Strength Test of the Steel Wire Rope. The residual strength of the steel wire rope is directly related to the cross-sectional area of the metal, so the detection of the residual strength of the steel wire rope can be realized by the LMA detection method [18]. After the wire rope is saturated and magnetized, when the cross-sectional area of the metal is lost, its internal magnetic flux will change. The change is detected by the induction coil; that is, the cross-sectional area of the wire rope can be detected by measuring the induced voltage at both ends of the detection coil [19]. When the excitation coil is energized, a variable MF is generated. The induced voltage generated in the detection coil can be determined by Faraday's law of electromagnetic induction:

$$u = -M\frac{\mathrm{d}\varphi}{\mathrm{d}t} = -ML\frac{\mathrm{d}B}{\mathrm{d}t}. \quad (1)$$

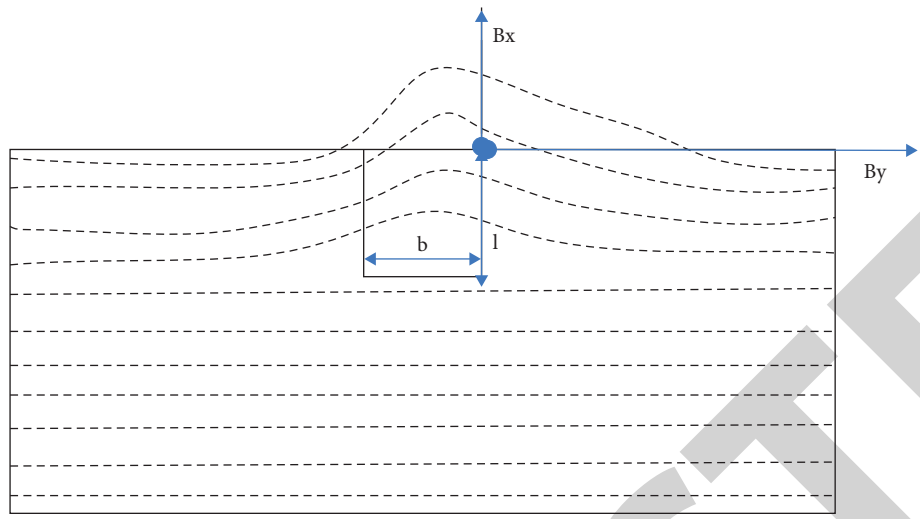

Figure 4: The characteristics of the leakage MF of the broken wire of a steel wire rope.

In the formula, M is the number of turns of the induction coil and L is the area occupied by the wire rope specimen in the excitation coil.

The magnetic flux density B can be obtained by integrating the time variable t on both sides of the above equation at the same time:

$$B = \frac{\mathrm{HU}}{\mathrm{ML}}. \tag{2}$$

In the formula, U is the integral voltage and H is the integral constant.

It is extremely difficult to quantitatively measure the magnetic flux in a steel wire rope. In order to map the change law of the metal cross-sectional area of the steel wire rope to the magnetic flux change in the steel wire rope, some indirect measurement methods are needed. This study adopts an improved main magnetic flux detection method [20].

The total magnetic flux φ_Z measured in the coil includes the magnetic flux φ_K in the air gap and the magnetic flux φ_G in the wire rope. The magnetic flux in the air gap passes between the inner side of the measuring detection coil and the surface of the wire rope, namely,

$$\varphi_Z = \varphi_K + \varphi_G. \tag{3}$$

According to Faraday's law of electromagnetic induction, when the magnetic flux becomes larger, the generated current has a tendency to make it smaller; while the magnetic flux becomes smaller, the generated current has a tendency to make it larger. The induced electromotive force of the detection coil is calculated as follows:

$$E = -\frac{\mathrm{d}(n\varphi_Z)}{\mathrm{d}t}. \tag{4}$$

In the formula, n is the number of turns of the detection coil.

Integrating both sides of equation (4) at the same time, we obtain

$$\int E\mathrm{d}t = -\int n\mathrm{d}\varphi_Z. \tag{5}$$

From equation (5), the output voltage of the integrator is obtained as U_0:

$$U_0 = nH\int \mathrm{d}\varphi_Z. \tag{6}$$

Substituting formula (3) into formula (6), we obtain

$$U_0 = nH\int \mathrm{d}(\varphi_K + \varphi_G). \tag{7}$$

The magnetic flux is obtained as the product of the magnetic induction intensity and the induction area, as follows:

$$\varphi = A \cdot B. \tag{8}$$

Then, the magnetic flux of the detection coil is obtained as follows:

$$\varphi_Z = (A \cdot B)_K + (A \cdot B)_G. \tag{9}$$

After replacing the integral, using the principle of differentiation, we can get

$$U_0 = nH\int [(A\cdot dB)_K + (A\cdot dB)_G + (B\cdot dA)_K + (B\cdot dA)_G]. \tag{10}$$

Expanding formula (10), we can get

$$U_0 = nH\int (A_K \cdot dB_K + A_G \cdot dB_G + B_K \cdot dA_K + B_G \cdot dB_G). \tag{11}$$

In the formula, A_K and B_K represent the cross-sectional area and magnetic induction intensity in the air gap of the detection coil, respectively; A_G and B_G, respectively, represent the metal cross-sectional area and magnetic induction intensity of the wire rope in the detection coil.

In the actual testing process, due to the loss of the metal cross-sectional area (broken wire, wear, corrosion, etc.), the

cross-sectional area of the wire rope is reduced. Therefore, in the cross-sectional area surrounded by the detection coil, the air gap increases. The area increases accordingly, so we get

$$dA_K = -dA_G. \tag{12}$$

Substituting formula (12) into formula (11), we get

$$U_0 = nH \int [A_K \cdot dB_K + A_G \cdot dB_G + (B_G - B_K)dA_G]. \tag{13}$$

Equation (13) performs integral processing to get

$$U_0 = nH[A_K \cdot B_K + A_G \cdot B_G + (B_G - B_K)\Delta A_G]. \tag{14}$$

In the formula, ΔA_G is the change in the cross-sectional area of the metal.

The sudden change of the wire rope output signal is produced by $(B_G - B_K)\Delta A_G$. It can be seen from equation (14) that the voltage output in the integrator has a linear relationship with the loss of the wire rope's metal cross-sectional area and has nothing to do with time. In the actual test, some wire ropes have different magnetic fields and strengths, so different parameters should be set in a targeted manner, so that the residual strength of the wire rope can be detected more accurately.

2.5. Design and Analysis of Excitation Parameters. The main basis for designing the excitation magnetic circuit is the law of the magnetic circuit. The law of the magnetic circuit is the basic principle for analyzing and calculating the structural parameters of the magnetic circuit, including Kirchhoff's first law, Kirchhoff's second law, and Ohm's law [21].

2.5.1. Kirchhoff's First Law. It is also known as the law of magnetic flux continuity. According to the law, the total amount of magnetic flux in the magnetic circuit remains unchanged, and the algebraic sum of the magnetic flux passing through any node in the magnetic circuit is zero. For any cross-section of the branch magnetic circuit, the magnetic flux entering the cross-section is always equal to the magnetic flux passing through the cross-section [22].

2.5.2. Kirchhoff's Second Law. The magnetomotive force generated by the excitation coil is equal to the sum of the magnetic voltage drops in each part of the magnetic circuit. The magnetic pressure drop in the magnetic circuit can be divided into three parts: the magnetic pressure drop of the detection part, the magnetic pressure drop of the measured section of the steel wire rope, and the magnetic pressure drop of the air gap. The equivalent magnetic circuit is shown in Figure 5.

Suppose their lengths are C_1, C_2, C_3 and the MF strengths are Q_1, Q_2, Q_3, respectively. Suppose each part is uniformly magnetized. The product of the MF strength Q and the magnetic path length C is the magnetic voltage drop of this section, then

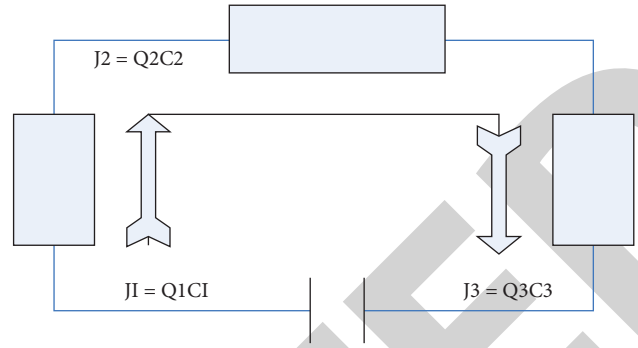

Figure 5: Isomagnetic circuit.

$$J_x = Q_x C_x. \tag{15}$$

If the number of turns of the excitation coil is S and the input current is I, the magnetomotive force generated by the excitation coil is SI.

The generated magnetomotive force is equal to the sum of the magnetic voltage drop of each part of the structure, and then,

$$\mathrm{SI} = C_1Q_1 + C_2Q_2 + C_3Q_3. \tag{16}$$

2.5.3. Ohm's Law. Assuming that the field strength is evenly distributed in the area where the coil is wound, and the cross-sectional area of the coil is M.

The magnetic flux φ passing through the coil is obtained as follows:

$$\varphi = BM = \mu QM. \tag{17}$$

For the coil itself, there is

$$nI = QC. \tag{18}$$

MF strength of the coil is obtained as follows:

$$Q = \frac{nI}{C}. \tag{19}$$

Substituting into equation (17), we get

$$\varphi = \frac{\mu M}{C} nI. \tag{20}$$

3. Experiment and Analysis

3.1. Introduction to Experimental Procedures

3.1.1. Building an Experimental Platform and Debugging the Testing Device. The design requirements of the wire rope experimental platform are to ensure high signal accuracy, reduce external interference, have a high signal-to-noise ratio and controllable experimental conditions, and allow repeated experiments. Based on the previous theoretical analysis, the detection platform is designed and the overall structure scheme is as follows: first, the signal generating device generates different types of signals with adjustable parameters (such as frequency and amplitude). The power

amplifier is connected to the excitation coil of the sensor, the data acquisition instrument is connected to the induction coil of the sensor, and the generated signal is amplified by the power amplifier and then input to the excitation coil of the sensor. According to electromagnetic theory, a changing voltage signal (such as an input pulse voltage) will produce a changing MF in a closed circuit, and the changing MF will produce a changing voltage. That is, with the continuous change of the input signal, the MF in the telescopic sensor will continue to change, and the corresponding electrical signal will be output in the induction coil. The electrical signal output is collected by the detection coil, the signal is input into the computer for processing and analysis, and finally the experimental data are obtained. The experimental data are recorded by the computer and cleaned and counted after the experiment, and then, the next step analysis is carried out on the SPSS software. Figure 6 shows a schematic diagram of the experimental process.

Under the condition that the change of the magnetic flux per unit time remains unchanged, increasing the number of turns of the induction coil can effectively improve the ability of the sensor to detect the magnetic characteristic parameters. However, if the number of turns of the detection coil is too large, the signal-to-noise ratio will decrease if it exceeds a certain range. When designing the detection coil, the detection coil is put on the test piece. The diameter of the detection coil should be larger than the diameter of the test piece. At the same time, in order to improve the signal-to-noise ratio of the signal, the distance between the coil and the test piece should not be too large. The diameter is 12 mm. According to the previous analysis, when the ratio of the coil length to the radius is at least 5, the coil attenuation coefficient is greater than 99%, and the coil can be regarded as an ideal coil [23]. Therefore, as shown in Figure 7, the length of the detection coil in the detection system needs to be greater than or equal to 40 mm. Taking into account other structural dimensions and mutual cooperation of the sensor, the length of the detection coil is taken as 85 mm.

3.1.2. Design and Manufacture of Steel Wire Rope Magnetic Parameter Detection Sensor. The sensor adopts a symmetrical split structure as a whole, which is easy to disassemble. As the diameter of the wire rope increases, the sensor structure will increase accordingly, and the size of each part of the structure must meet the minimum size that makes the wire rope magnetized to saturation. By establishing simulation models of wire ropes with different diameters and simulating the damage MF, the reasonable size of each part can be obtained. Table 1 lists the dimensions of each part of the wire rope excitation structure when the diameter is different.

According to the size table of each part, the housing structure of the wire rope damage detection sensor is designed and manufactured, and a through hole is designed at the top and bottom of the sensor to lead out the power line, signal line, etc. There are two grooves in each of the upper and lower parts for installing the detection circuit board. The finished circuit board is wired and fixed it in the groove, then the permanent magnets are attached to the round holes on both sides of the sensor, and the upper and lower parts are fixed with a semicircular iron sheet. Figure 8 shows an assembly structure diagram of the excitation structure, the permanent magnet, the steel wire rope, and the detection circuit board.

The layout of the sensor is shown in Figure 9. The excitation sensor consists of an excitation coil and a coil bias magnetizer. The number of turns of the excitation coil is 38, which is made of enameled wire with a diameter of 0.45 mm. The number of turns of the coil bias magnetizer is 900 turns, which is made of enameled wire with a diameter of 1 mm. The receiving sensor is composed of a permanent magnet bias magnetizer and a receiving coil. The number of turns of the receiving coil is 30, which is made of enameled wire with a diameter of 0.45 mm. In the experiment, the position of the receiving sensor is fixed. Firstly, the excitation sensor is installed at position 1, and the relationship between the energy conversion efficiency of the steel wire magnetostrictive guided wave in the excitation process of the fatigue zone and the bias intermediate frequency intensity is obtained. Then, the excitation sensor is installed at position 2, and the relationship between the energy conversion efficiency of the wire magnetostrictive guided wave excitation process and the bias MF intensity in the non-fatigue region is obtained.

3.1.3. Making Experimental Specimens. In this experiment, steel rods with diameters of 6 mm, 8 mm, and 10 mm were selected as the experimental specimens. The steel rod specimens just received will have partial magnetism. In order to prevent this magnetism from interfering with the experiment, it needs to be demagnetized first. Common demagnetization methods include heating demagnetization and alternating current demagnetization. The heating demagnetization method is to heat the test piece to the Curie temperature and then cool it. This method requires a lot of equipment and takes a long time, so this method is not used in this experiment. In this experiment, the AC excitation method is selected for the demagnetization of the steel rod specimen. The AC demagnetization method is to pass an alternating current into the excitation coil, so that the direction of the external MF of the steel rod specimen is continuously changed, and at the same time, the MF strength is gradually reduced to achieve demagnetization. Effectively, this method is convenient, fast, and suitable for this experiment [24].

3.2. Data Analysis. LMA is used to show the percent equivalent curve of metal cross-section loss due to rust, wear, wire breakage, fatigue, etc. for ferromagnetic substances. The root cause of steel wire rope LMA type damage is the reduction of the effective cross-sectional area. From the outside, it is the decrease of the cross-sectional area due to wear and other reasons. From the inside, there is material deterioration and fatigue damage caused by long-term use, as follows:

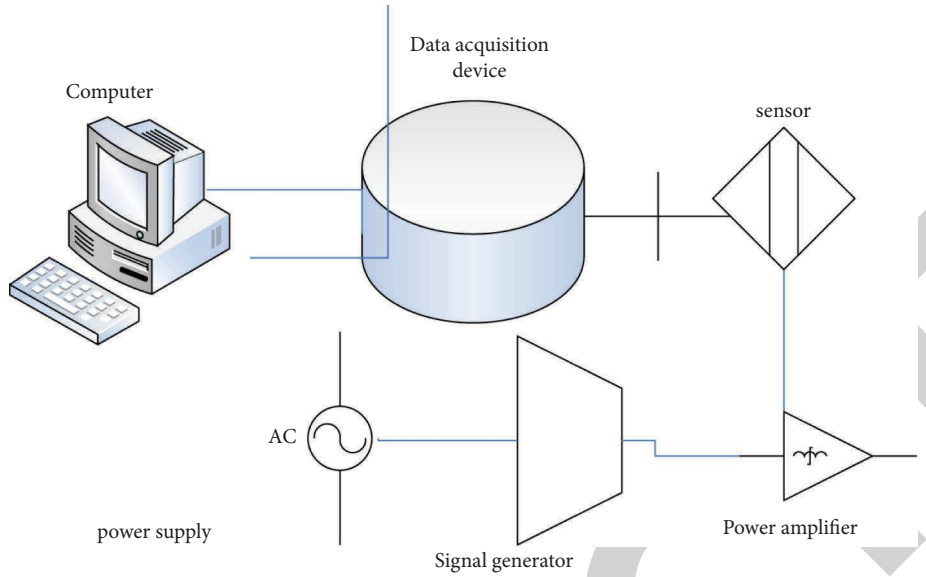

Figure 6: The overall scheme of the experimental system.

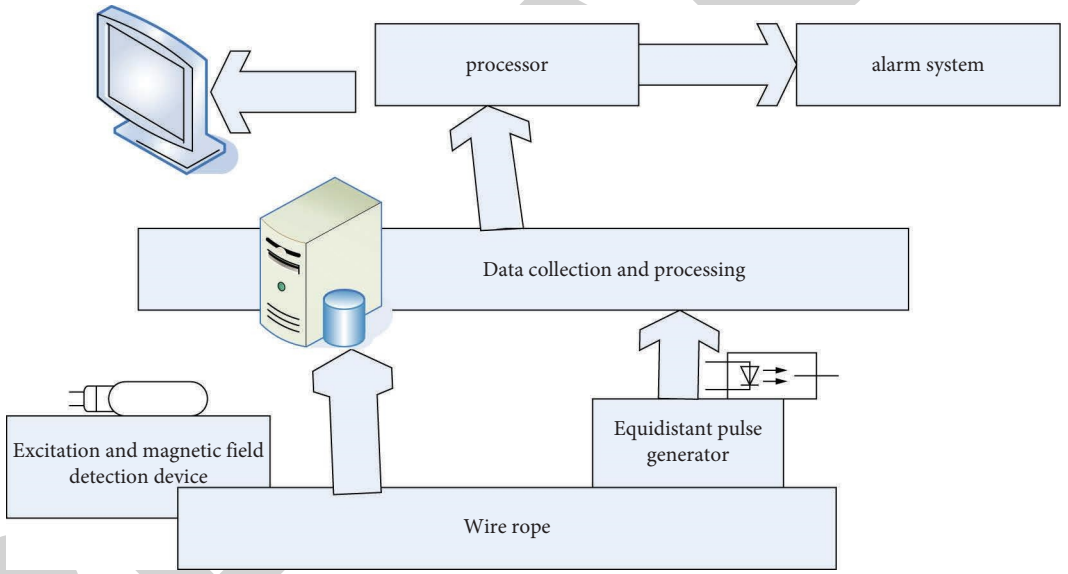

Figure 7: The structure diagram of the detection system.

Table 1: Dimensions of each part of the sensor.

Sensor structure parameters						
Wire diameter	Internal distance of armature	Radial thickness of armature	Distance between wire rope and armature inside	Axial length of permanent magnet	Radial length of permanent magnet	Air gap
8	40	2	30	15	25	3
16	60	4	30	15	25	3
32	75	4	40	15	25	3
40	90	6	40	15	25	3

(1) The reduction in cross-sectional area leads to a decrease in residual strength due to wear and the decrease in the cross-sectional area of the wire rope and the residual strength. In order to simulate this situation, steel rods with different cross-sectional areas are selected for comparative experiments. The purpose is to observe and analyze the change law of magnetic parameters after the cross-sectional area is reduced.

Figure 8: Wire rope damage detection device.

(2) Internal fatigue damage leads to a decrease in residual strength due to long-term use and fatigue damage occurs inside the wire rope, which manifests as small internal cracks. Although it cannot be found on the surface, the residual strength of the wire rope has actually decreased. In order to simulate this situation, the steel rods were stretched for multiple simulations to cause fatigue damage inside the steel rods, thereby fabricating specimens with different residual strengths. The purpose is to observe and analyze the change law of magnetic parameters after internal fatigue damage occurs [25].

The steel rod specimens with diameters of 6 mm, 8 mm, and 10 mm were used for testing. The test results are listed in Table 2. It can be seen from the results that as the cross-sectional area increases, the remanence and coercive force tend to increase. This is because in the magnetic circuit, the larger the cross-sectional area of the test piece means the stronger the magnetic permeability, which results in the detection of greater remanence and saturation magnetic induction.

Using a steel rod specimen with a diameter of 10 mm is cyclically stretched on a tensile testing machine with a tensile force of 60 kN, and the saturation magnetic induction and remanence are obtained, as listed in Table 3.

It can be seen from the results in Table 3 that during the cycle, the more cycles, the smaller the breaking force. After the first two cycles, the remanence and saturation magnetic induction of the wire rope decrease by a large extent. During the first to 17th cycles, the remanence and saturation magnetic induction of the wire rope have a smaller amplitude. This is because at the beginning of stretching, the main reason for the change of the magnetic parameters is that the specimen becomes thinner due to the stretching. In the subsequent cycle, the diameter of the specimen changes very little. The reason for the change of the magnetic parameters is the internal material deterioration [26, 27]. Therefore, in the tensile link of the experiment, the steel wire rope showed relatively excellent performance, and in terms of residual strength, the magnetic induction intensity of the steel wire rope was small.

In the experiment, a steel rod specimen with a diameter of 10 mm was selected to test its magnetic parameters without tensile fatigue. After the input current value and output voltage value are obtained, the input current value and the voltage signal received by the computer are processed to obtain the MF intensity and magnetic induction intensity of the test piece, as listed in Table 4.

The analysis result shows that even if the current value continues to increase, the output voltage will hardly increase; that is, the test piece has been magnetized to saturation. In order to obtain further magnetic parameters, the saturated test piece is magnetized in reverse. After getting enough data, the drawn hysteresis loop is shown in Figure 10.

In order to simulate the fatigue damage of the steel wire rope, a steel rod specimen with a diameter of 10 mm was used, and the tensile force was gradually loaded to 70 kN using a tensile testing machine and then restored, and the load was repeated 900 times to cause fatigue damage inside the specimen. The magnetic parameter detection platform is used to detect the magnetic parameters of the test piece and draw its hysteresis loop. The hysteresis loops of the untreated samples with a diameter of 10±mm were integrated into one picture, as shown in Figure 10.

It can be seen from Figure 10 that the hysteresis loop diagrams of the two are obviously different: compared with the specimens without fatigue stretching, the hysteresis loops of the specimens subjected to fatigue stretching are more "short." The reason is that with the gradual intensification of fatigue damage, microcracks start to grow inside the material. These microcracks will further expand. A small number of grains inside the material will break down to form subgrains, resulting in a decrease in permeability due to increased dislocations. The saturation magnetic flux density and remanence are reduced, and at the same time, due to the deterioration of the material, it is more difficult for the specimen to be magnetized to the saturation state [28].

Finally, three types of steel wire ropes with different cross-sectional area damage levels are designed through modeling software, among which Figure 11(a) shows the intact steel wire rope as the reference object, Figure 11(b) shows the wire rope single strand with a defect depth of 2 mm and a defect width of 2 mm, and Figure 11(c) shows a single strand of broken wire for the steel wire rope, and the width of the defect is 2 mm, as shown in Figure 11.

The lift-off value of the steel wire rope is taken as 0.5 mm along the circumference of the steel wire rope as the reflection path of the leakage MF.

Analyzing Figure 12, the detection device detects obvious changes in the leakage MF at the damage of the steel wire rope, and the magnetic flux density of the leakage MF generated after a single strand of the wire rope is broken is much larger than the magnetic flux density of the leakage MF generated by the single strand of the wire rope. It shows that the magnetic flux density value of the steel wire rope leakage field increases with the increase of the metal cross-sectional area loss of the steel wire rope. Therefore, the excitation detection device designed in this section can

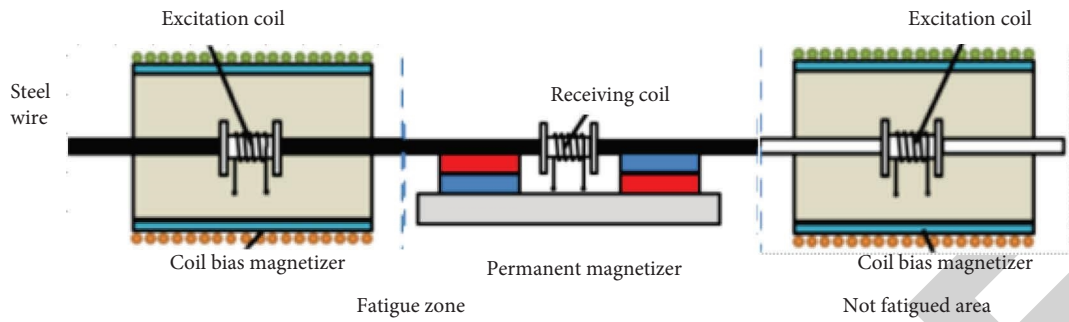

Figure 9: Sensor layout.

Table 2: The relationship between the cross-sectional area of the test piece and the voltage.

Cross-sectional area	Voltage	Remanence	Saturation magnetic induction	Breaking force
52.13	97.6	764.8	2211.3	51.1
84.20	112.5	781.9	2754.2	66.4
117.64	133.9	796.1	2943.5	79.8

Table 3: The relationship between fatigue damage and magnetic parameters.

Cycles	Saturation magnetic induction	Remanence	Residual strength
1	2176.4	771.3	70.2
3	2173.2	766.8	67.3
5	2171.8	763.5	65.5
7	2170.1	761.4	63.1
9	2168.3	760.2	62.2
11	2164.9	759.3	61.4
13	2162.1	757.6	60.6
15	2160.7	755.8	59.3
17	2158.5	753.7	58.0

Table 4: The relationship between MF intensity and magnetic induction intensity.

Cycles	Input current	MF strength	Output voltage	Magnetic induction
1	0	0	0	0
2	0.05	288	10.5	239.1
3	0.10	576	12.3	255.2
4	0.15	633	15.4	269.4
5	0.20	730	17.2	280.5
6	0.25	805	18.8	298.7
7	0.30	862	19.7	305.2
8	0.35	910	20.3	314.6
9	0.40	1120	30	372
10	0.45	1630	30	372

realize the detection of wire rope cross-sectional area damage. It shows that the excitation device optimized based on simulation can well meet the wire rope excitation requirements and has a good magnetization effect [29].

4. Discussion

The wire rope specimens with cross-sectional area loss ratios of 0.036, 0.089, and 0.115 were simulated, and the wire rope specimens were subjected to 2, 4, 6, 8, and 10 kN tensile forces respectively, and the same damage and different tensile forces were simulated and analyzed. In this paper, the distribution and variation law of stress and strain of different damaged wire rope samples under the action of external tension, as well as the variation law of local stress and strain are analyzed. Based on the simulation data, this paper also analyzes the corresponding relationship between the applied tension and strain and the applied tension and stress. According to the calculation results of the residual strength based on strain and stress under different section loss ratio conditions, the corresponding relationship between the residual strength of the steel wire rope and the section loss ratio is solved; the residual strength based on strain and stress is compared and analyzed, and the residual strength is

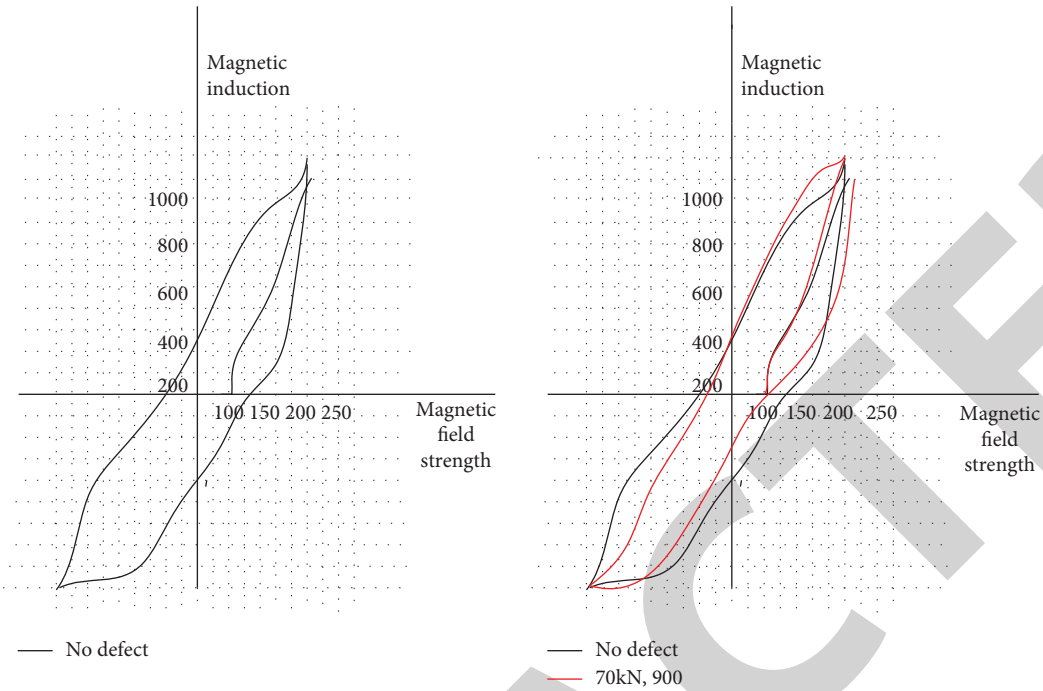

Figure 10: The hysteresis loop changes under different pressures.

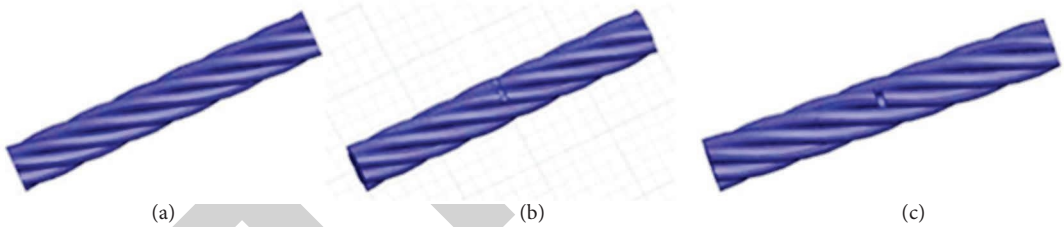

Figure 11: Three wire rope models with different degrees of damage.

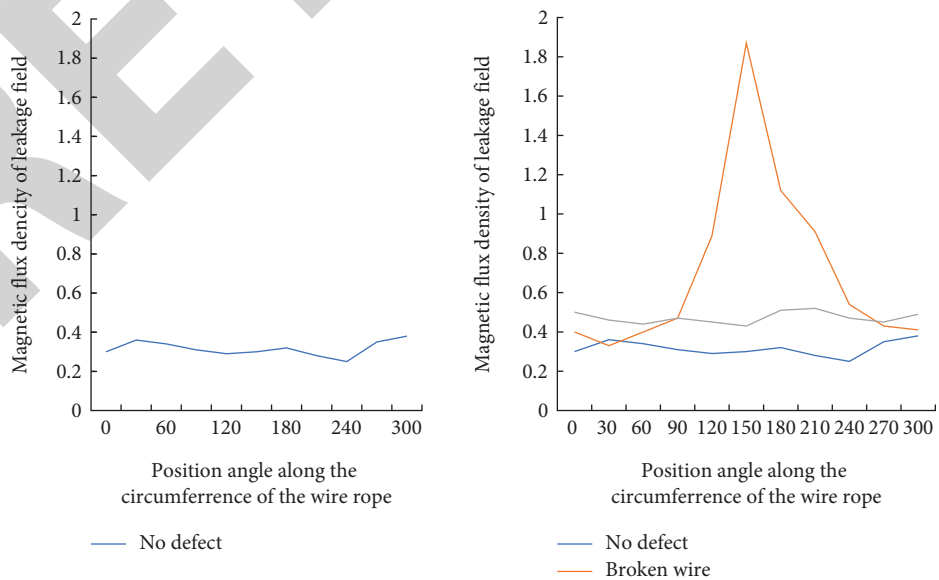

Figure 12: The change curve of the leakage MF at the damage of three different steel wire cross-sectional areas with a lift-off value of 0.5 mm.

given The selection method of the safe service tension solution of the steel wire rope is based on reference [30]. By drawing the hysteresis loop diagrams of steel rods with different degrees of fatigue damage, it can be found that the hysteresis loop diagram can reflect the fatigue damage of the steel rod specimen to a certain extent. It can be seen that the hysteresis loop method is feasible as a method of magnetic detection of the residual strength of a steel wire rope. The excitation effect and detection performance simulation analysis of the wire rope magnetization detection sensor is carried out. The analysis results show that the sensor has a good excitation effect and detection effect, and the detection sensitivity exceeds 85%.

5. Conclusion

The purpose of wire rope nondestructive testing is to evaluate the residual strength of the wire rope based on the metal cross-sectional area loss detection, combined with the actual operating state and conditions of the wire rope, to provide guidance for the reasonable, safe, and effective application of the wire rope [31]. This experiment demonstrates that the magnetic sensor can effectively detect wire rope defect changes in theory, with strong feasibility and high sensitivity. However, there is still room for further improvement in the field of wire rope residual strength detection. For example, on-site wire rope defect signal detection can be studied. By further optimizing the detector, it can reduce the impact of complex environment on the site, reduce vibration, and improve the quality of wire rope defect signal acquisition [32]. At the same time, a practical and efficient signal processing method can be found to realize the quantitative detection of the residual strength of the wire rope. Through in-depth research on the principle of residual strength detection of steel wire ropes, the corresponding judgment standards and methods are formulated. The wire rope excitation device needs to be optimized to further improve the excitation effect to improve the accuracy and accuracy of detection. The actual working conditions are much more complicated than the laboratory environment. To apply the entire system to engineering practice, more in-depth experiments and research are required [33, 34].

Data Availability

The data that support the findings of this study are available from the corresponding author upon reasonable request.

Conflicts of Interest

The authors declare that they have no conflicts of interest.

Acknowledgments

This research was financially supported by the project of the Intelligent Transportation Traffic Control System of Mine Ramp Road in 2022 (2022GY0004).

References

[1] H. Wang, J. Tian, X. Li, and X. Lv, "Inspection of mine wire rope using magnetic aggregation bridge based on magnetic resistance sensor array," *IEEE Transactions on Instrumentation and Measurement*, vol. 69, no. 10, pp. 7437–7448, 2020.

[2] M. Trinidad, "In-situ steel wire rope inspection utilising MFL," *Non Destructive Testing Australia*, vol. 5, no. 5, pp. 31–34, 2018.

[3] H. Tom, "Residual field MFL - wire rope inspection, removing risk & uncertainty," *Industrial Eye: The Official Journal of the Australian Institute for Non-Destructive Testing*, vol. 4, no. 4, pp. 34-35, 2017.

[4] P. Zhou, G. Zhou, Y. Li, Z. He, and Y. Liu, "A hybrid data-driven method for wire rope surface defect detection," *IEEE Sensors Journal*, vol. 20, no. 15, pp. 8297–8306, 2020.

[5] Z.-Y. Tian, J.-W. Tan, and Y. Wen, "The signal processing technology of stubble in steel rope," *Industry and Mine Automation*, vol. 32, no. 4, pp. 13–15, 2006.

[6] U. Pal, G. Mukhopadhyay, A. Sharma, and S. Bhattacharya, "Failure analysis of wire rope of ladle crane in steel making shop," *International Journal of Fatigue*, vol. 116, pp. 149–155, 2018.

[7] B. Yu, J. W. Kim, and S. Park, "Magnetic-flux-leakage-based pressure deformation detection of elevator wire rope," *Journal of the Korean Society for Nondestructive Testing*, vol. 37, no. 4, pp. 269–275, 2017.

[8] V. Fontanari, C. Menapace, and E. Pedrotti, "Study of the lightning damage produced in a full-locked wire rope of an aerial cableway," *Engineering Failure Analysis*, vol. 103, pp. 530–539, 2019.

[9] J. Tian, Y. Hu, H. Guo, and C. Zhao, "Research on mine-used wire rope flaw detector based on Hall element," *Industry and Mine Automation*, vol. 45, no. 11, pp. 75–80, 2019.

[10] D. Zhang, C. Feng, K. Chen, D. Wang, and X. Ni, "Effect of broken wire on bending fatigue characteristics of wire ropes," *International Journal of Fatigue*, vol. 103, pp. 456–465, 2017.

[11] G. Shen, Y. Zheng, Z. Jiang, and J. Tan, "The development status of magnetic Barkhausen noise technology," *Nondestructive Testing*, vol. 38, no. 7, pp. 66–74, 2016.

[12] H. Wang, X. Li, Y. Han, and L. Xin, "Design of damage detection system for mine-used wire rope," *Industry and Mine Automation*, vol. 46, no. 6, 2020.

[13] W. Wang, "Acoustic emission detection technology for pressure pipeline leakage," *Non-Destructive Testing*, vol. 38, no. 3, pp. 22–24, 2016.

[14] S. Liu and F. Liu, "Non-destructive testing technology and its progress in the aviation industry," *Non-Destructive Testing*, vol. 39, no. 6, pp. 56–60, 2017.

[15] Z. Wang, X. Bu, and W. Han, "Fast unfolding and stitching of defect images in shaft surface fluorescent magnetic particle inspection," *Nondestructive Testing*, vol. 40, no. 1, pp. 1–5, 2018.

[16] Y. Yang, D. Li, and P. Yang, "Acoustic emission feature extraction for rolling bearing faults based on parameter analysis," *Nondestructive Testing*, vol. 40, no. 1, pp. 6–10, 2018.

[17] X. Sun, S. Jin, D. Zhang et al., "TOFD quantitative detection of small cracks based on autoregressive spectrum extrapolation," *Nondestructive Testing*, vol. 39, no. 10, pp. 8–11, 2017.

[18] W. Guo, L. Dong, B. Xu, and T. Qu, "Research status and progress of active infrared thermal imaging nondestructive testing technology," *Nondestructive Testing*, vol. 38, no. 4, pp. 58–66, 2016.

[19] L. Dou, W. Zhan, and X. Bai, "Damage identification of broken wires inside and outside the wire rope," *Industry and Mine Automation*, vol. 47, no. 3, pp. 83–88, 2021.
[20] J. Ren, H. Liu, and K. Song, "The rise and development of metal magnetic memory testing technology," *Nondestructive Testing*, vol. 38, no. 11, pp. 7–15, 2016.
[21] L. Peng, "Design of intelligent parking management system based on geomagnetic sensor," *Control Engineering*, vol. 23, no. 8, pp. 1295–1300, 2016.
[22] G. Shi, X. Li, X. Li, Y. Liu, R. Kang, and X. Shu, "The equivalent two-step method for calibration of three-axis magnetic sensor in heading measurement system," *Chinese Journal of Scientific Instrument*, vol. 38, no. 2, pp. 402–407, 2017.
[23] W. Li, X. Guan, M. Yang, W. Jiang, and H. Zhang, "High-rotation speed measurement system based on magneto-resistive sensor," *Electronic Measurement Technology*, vol. 2, no. 2, pp. 180–183, 2017.
[24] J. Wang, W. Song, R. Yi, Q. Song, and S. B. Corp and Ltd, "Application research of magnetoresistive sensors in electronic water meters and gas meters," *Integrated Circuit Applications*, vol. 4, no. 4, pp. 42–44, 2017.
[25] D. Chen, M. Pan, W. Tian, W. Zhou, and R. Xie, "Detection of micro-defects in engine blades based on flexible electromagnetic sensors," *China Testing and Testing*, vol. 44, no. 1, pp. 65–68, 2018.
[26] X. Sun, "Discussion on the detection and maintenance of elevator hoisting machinery wire ropes," *Science Technology and Enterprise*, no. 4, p. 241, 2016.
[27] Z. Ren, Z. Yu, and X. Chen, "Study on wire rope elastic-plastic damage constitutive model," *Journal of Mechanical Engineering*, vol. 53, no. 1, pp. 121–129, 2017.
[28] J. Ma, P. Guo, B. Zhang, B. Xu, and Z. Wang, "Manufacturing technology and quality control of riding slings for steel wire ropes of Qingshuihe Bridge," *Highways*, vol. 62, no. 4, pp. 113–117, 2017.
[29] X. Zhao, H. Wang, C. Fu, W. Cui, P. Zhao, and X. Tian, "Research on the unfolding line of braided anti-twist steel wire rope and its mechanical modeling," *Mechanical Strength*, vol. 39, no. 1, pp. 111–116, 2017.
[30] W. Zhou, "Research progress on the breaking and tearing mechanism and detection methods of steel cord conveyor belts used in coal mines," *China Science and Technology*, no. 23, pp. 89-90, 2016.
[31] J. Wang, "Analysis and preventive measures of port crane wire rope fracture accident," *Science and Technology*, no. 5, p. 129, 2017.
[32] M. Zhang, Z. Kou, and L. Ting, "Wire rope torque analysis based on ABAQUS," *Coal Mine Safety*, vol. 47, no. 2, pp. 113–115, 2016.
[33] X. Gong, Y. Luo, and S. Wu, "The influence of hoist drum structure on the deformation and detuning of multi-layer winding double steel wire rope," *Journal of China Coal Society*, vol. 41, no. 8, pp. 2121–2129, 2016.
[34] L. Cao and Z. An, "Comparative study of BP and RBF neural network in the prediction of the number of broken wires in crane wire ropes," *Coal Mining Machinery*, vol. 37, no. 1, pp. 193–195, 2016.